Bioactive Materials 6 (2021) 627–637

Contents lists available at ScienceDirect

Bioactive Materials

journal homepage: http://www.keaipublishing.com/biomat

Neuro-regenerative imidazole-functionalized GelMA hydrogel loaded with hAMSC and SDF-1α promote stem cell differentiation and repair focal brain injury

Yantao Zheng[a,1], Gang Wu[b,1], Limei Chen[c], Ying Zhang[c], Yuwei Luo[d], Yong Zheng[e], Fengjun Hu[f], Tymor Forouzanfar[g], Haiyan Lin[h,*], Bin Liu[a,c,**]

[a] Emergency Department, Zhujiang Hospital, Southern Medical University, Guangzhou, China
[b] Department of Oral Implantology and Prosthetic Dentistry, Academic Centre for Dentistry Amsterdam (ACTA), University of Amsterdam (UvA) and Vrije Universiteit Amsterdam (VU), Amsterdam, Netherlands
[c] Department of Emergency, Guangzhou Red Cross Hospital, Medical College, Jinan University, Guangzhou City, 510220, China
[d] Rheumatology Department, The Third Affiliated Hospital of Southern Medical University, Guangzhou, China
[e] Emergency Medicine Department, Qingxin Section of Qingyuan People's Hospital, Qingyuan, China
[f] Institute of Information Technology, Zhejiang Shuren University, Hangzhou, China
[g] Department of Oral and Maxillofacial Surgery/Pathology, Amsterdam UMC and Academic Center for Dentistry Amsterdam (ACTA), Vrije Universiteit Amsterdam, Amsterdam Movement Science, de Boelelaan, 1117, Amsterdam, Netherlands
[h] Savaid Stomatology School, Hangzhou Medical College, Hangzhou, China

ARTICLE INFO

Keywords:
Injectable hydrogel
Imidazole
Stromal-cell derived factor-1 (SDF-1α)
Human amniotic mesenchymal stromal cells (hAMSCs)
Brain injury

ABSTRACT

Brain tissues that are severely damaged by traumatic brain injury (TBI) is hardly regenerated, which leads to a cavity or a repair with glial scarring. Stem-cell therapy is one viable option to treat TBI-caused brain tissue damage, whose use is, whereas, limited by the low survival rate and differentiation efficiency of stem cells. To approach this problem, we developed an injectable hydrogel using imidazole groups-modified gelatin methacrylate (GelMA-imid). In addition, polydopamine (PDA) nanoparticles were used as carrier for stromal-cell derived factor-1 (SDF-1α). GelMA-imid hydrogel loaded with PDA@SDF-1α nanoparticles and human amniotic mesenchymal stromal cells (hAMSCs) were injected into the damaged area in an *in-vivo* cryogenic injury model in rats. The hydrogel had low module and its average pore size was 204.61 ± 41.41 nm, which were suitable for the migration, proliferation and differentiation of stem cells. *In-vitro* cell scratch and differentiation assays showed that the imidazole groups and SDF-1α could promote the migration of hAMSCs to injury site and their differentiation into nerve cells. The highest amount of nissl body was detected in the group of GelMA-imid/SDF-1α/hAMSCs hydrogel in the *in-vivo* model. Additionally, histological analysis showed that GelMA-imid/SDF-1α/hAMSCs hydrogel could facilitate the regeneration of regenerate endogenous nerve cells. In summary, the GelMA-imid/SDF-1α/hAMSCs hydrogel promoted homing and differentiation of hAMSCs into nerve cells, and showed great application potential for the physiological recovery of TBI.

1. Introduction

Brain, as one of the most delicate organs, is responsible for language, behavior and various neuroregulatory functions [1]. Brain injury, caused by traumatic brain injury (TBI) or stroke, may severely affect nervous system, subsequently causing dysfunction for patients and even threatening their lives [2]. Brain tissue bears very limited self-healing capacity and it has nearly no potential to regenerate lost parts [2–4]. Nerve cells and extracellular matrix (ECM) in the injured sites will be soon phagocytosed and removed, finally forming a cavity filled with extracellular fluid in brain [5] and surround by glial scarring [3]. This kind of irreversible damage eventually causes permanent function loss of the relevant brain area.

Tremendous treatment options have been attempted to treat TBI,

Peer review under responsibility of KeAi Communications Co., Ltd.
* Corresponding author.
** Corresponding author. Emergency Department, Zhujiang Hospital, Southern Medical University, Guangzhou, China
E-mail addresses: lhaiyanlily@163.com (H. Lin), nysylb@163.com (B. Liu).
[1] These authors contributed equally to the present research.

https://doi.org/10.1016/j.bioactmat.2020.08.026
Received 27 May 2020; Received in revised form 27 August 2020; Accepted 27 August 2020

among which stem cell replacement therapy is considered as a promising way to regenerate brain tissue [5]. Human amniotic mesenchymal stromal cells (hAMSCs) have attracted much attention since they are easily obtained without minimal ethical controversy [6,7]. Francesca et al. have found that hAMSCs showed neuronal rescue and introduction of trophic factors in TBI, which are favorable to protect brain [8]. Other researchers have found that hAMSCs treated-TBI present a significant decrease of microglia activation [6], as well as upregulation of vascular endothelial growth factor (VEGF) and brain-derived neurotrophic factor (BDNF) [9]. These results indicate that hAMSCs have great potential to protect the injured brain, reduce the loss of neurons, increase the expression of nutritional factors, and partially restore brain function.

In addition to using exogenous stem cell transplantation, it is also important to promote the migration of endogenous neural stem cells to the injured area to treat TBI. Stromal cell-derived factor-1 (SDF-1α) is one of the most attractive chemo attractants to promote stem cell homing [10,11]. SDF-1α can stimulate the proliferation rate of neuroblasts and promote its migration into injured areas. Besides, SDF-1α expression is widely detected in brain, participating in brain development, angiogenesis, and neurogenesis [12]. Polyphenol-based nanoparticles, such as polydopamine, can interact with biomolecules through non-covalent interactions, thereby carrying and slowly-releasing bioactive agents [13].

Injectable hydrogels are highly suitable for the treatment of TBI [1,14,15], since its injection can minimize the damage to the skull and ensure the direct access of its-carried medicine to the lesion [16]. In addition, hydrogels can be carriers for various bioactive elements, such as stem cells, cytokines and drugs. They also simulate the extracellular matrix (ECM) to provide a suitable environment for cell migration and proliferation [17,18]. Gelatin methacrylate (GelMA), containing cell adhesion-stimulating RGD peptide, is one of the most commonly used hydrogels for stem cell carrier [19,20]. Furthermore, it is also very important to promote the differentiation of stem cells. Imidazole molecules are proved to promote the differentiation of pluripotent stem cells into neural cells [21]. It is also found that hydrogel containing imidazole groups can repair spinal cord injury by promoting ECM remodeling [22]. Considering the effect of imidazole groups on stem cells, we decided to introduce imidazole groups into GelMA to promote the differentiation of hAMSCs.

In this study, we aimed to prepare an injectable hydrogel carrying hAMSCs to treat the TBI. The GelMA functionalized with imidazole groups (GelMA-imid) was used to load hAMSCs and promote their differentiation. The hydrogel was formed by blue light initiation and 2-mercapto-1-methylimidazole could react with GelMA by “click-chemistry” during the hydrogel formation process. In addition, polydopamine (PDA) was used to carry SDF-1α and loaded into the GelMA-imid hydrogel. This is the first time that imidazole molecules were covalently bond with GelMA to form hydrogel. *In-vitro* cell migration and differentiation experiments were used to evaluate the functions of SDF-1α and imidazole groups. The prepared GelMA-imid/SDF-1α/hAMSCs hydrogel was finally used to treat TBI rat model established by cryogenic injury. (see Scheme 1) We believed that the GelMA-imid/SDF-1α/hAMSCs hydrogel would be a prospective material to prevent nerve cells decrease and promote tissue regeneration in the injured area Scheme 1.

2. Materials and methods

2.1. Materials

Gelatin (type A, from porcine skin) was purchased from Sigma-Aldrich, USA. Methacrylic anhydride, 2-mercapto-1-methylimidazole were purchased from Macklin, China. Dopamine hydrochloride and sodium hydroxide were purchased from Aladdin, China. Recombinant human SDF-1α was purchased from Peprotech, USA. Phosphate buffered saline (PBS, pH = 7.4) and fetal bovine serum were purchased from Gibco, USA. Cell counting kit-8 (CCK-8) was purchased from Beyotime Biotechnology, China. LIVE/DEAD cell imaging kit was purchased from Thermal Fisher, USA. Bone wax was purchased from Guangzhou Beogene Biotechnology Co., Ltd. Guangzhou, China. All the other reagents were analytical grade and used without further purification.

2.2. Synthesis of PDA and PDA@SDF-1α nanoparticles

PDA nanoparticles were synthesized from previous reported methods [23]. Briefly, dopamine hydrochloride (180 mg) was dissolved in 90 mL of deionized water, then 0.8 mL of freshly prepared 1 M NaOH solution was added to the solution. The reaction mixture was stirred for 5 h at 50 °C. After that, the black suspension was centrifuged at 10,000 rpm for 30 min to obtain the precipitant. Washed the precipitant with deionized water for three times to remove the unreacted reagent. Lyophilized the precipitant to get the PDA nanoparticles.

The PDA@SDF-1α nanoparticles were obtained through non-covalent interactions between polydopamine and SDF-1α. In brief, SDF-1α (0.5 μg) was dissolved in 1 mL of PDA solution (1 mg/mL) and stirred for 24 h at 4 °C and lyophilized, the obtained PDA@SDF-1α nanoparticles was stored at −20 °C until use to protect its bioactivity.

2.3. Synthesis of GelMA

The GelMA was synthesized by a typical amide reaction [24]. Gelatin was dissolved in PBS buffer to obtain a 10% (w/v) solution. Methacrylic anhydride was added dropwise to the gelatin solution at a mass ratio of 0.6:1. The two-phase mixed solution was stirred at 50 °C for 1 h then dialyzed against deionized water for 3 days at 45 °C (MwCO = 3500). Next, the solution was centrifuged at 5000 rpm for 5 min to obtain the supernatant. Finally, stored the supernatant at −80 °C overnight and freeze-dried to obtain GelMA. The final product was stored at −20 °C until use.

2.4. Preparation of hydrogels

The GelMA-imid hydrogel was formed by blue light (405 nm) irradiation and 2-mercapto-1-methylimidazole was grafted to the gelatin molecular by click-chemistry [25,26]. GelMA was dissolved in PBS water to obtain a 5% solution, 2-mercapto-1-methylimidazole was dissolved in GelMA solution to form a concentration at 0%, 0.5%, 1% and 2%. LAP was added to the solution at a final concentration of 0.1% [27]. The hydrogel was finally formed by blue light (405 nm) irradiation for 30s. As for GelMA-imid/SDF-1α, GelMA-imid/hAMSC and GelMA-imid/SDF-1α/hAMSC hydrogels, the concentration of PDA@SDF-1α was 1 mg/mL, which contains 500 ng/mL SDF-1α; and the density of hAMSC was 1×10^5 cells mL^{-1}.

2.5. Characterization of the GelMA-imid hydrogel

Fourier transform infrared spectroscopy (FTIR, VERTEX70; Bruker, German) was used to analyze the chemical construction of Gelatin, GelMA and GelMA-imid. The test was executed in transmittance mode with KBr plates at a scanning wavelength from 400 cm^{-1} to 4000 cm^{-1} and a resolution of 4 cm^{-1}. Gelatin and lyophilized GelMA were rehydrated in D_2O and characterized by proton nuclear magnetic resonance (^1H NMR, Bruker AVAVCE 600 Hz; Bruker, German). The morphology of the lyophilized hydrogel was investigated by scanning electron microscopy (SEM, S-3400; Hitachi, Japan) at 5 kV. The rheological properties of hydrogel were tested by rotary rheometer (Kinexus Pro; Malvern, the UK). The experiments were carried on a parallel-plate (20 mm diameter) geometry. The stiffness of these hydrogel was measured by a time sweep test with a constant strain of 1% and frequency of 1 Hz at 25 °C. The stability of these hydrogels was measured by a

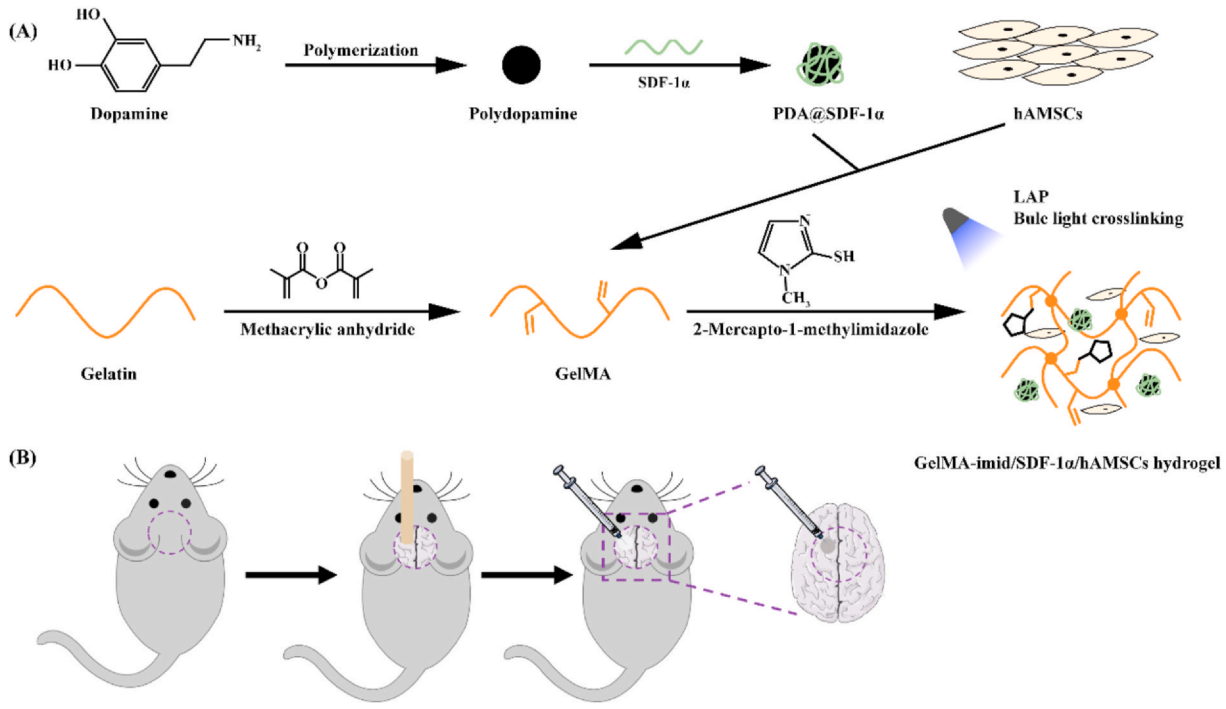

Scheme 1. (A) Illustration of GelMA-imid/SDF-1α/hAMSCs hydrogel preparation process. (B)Schematic diagram of establishing cryogenic injury model.

frequency sweep test with a constant strain of 0.5% and changing frequency from 0.1 Hz to 10 Hz at 25 °C. The shear thinning property was measured at a constant frequency of 0.1 Hz and 100 Hz at 25 °C. The mechanical property was tested by universal testing machine (Electro Force 3220; BOSE, USA) at a strain of 60% and compression rate of 0.05 mm s^{-1}.

2.6. In vitro degradation rate of the hydrogel

To analyze the *in vitro* degradation behavior of hydrogel, the cylindrical hydrogel was immersed in PBS buffer, and the weight of the hydrogel was recorded at a selected time [28]. The PBS buffer was changed after each weighing, and the hydrogel continued to soak under the previous conditions until it completely degraded. The degradation rate was calculated by formula: $\frac{W_t}{W_0} \times 100\%$. Where W_0 was the original weight of the hydrogel and W_t was the weight of the hydrogel at a selected time. Each sample was tested for three times.

2.7. Characterization of the PDA and PDA@SDF-1α nanoparticles

The morphology and size of PDA and PDA@SDF-1α nanoparticles were characterized by transmission electron microscopy (TEM, H-800; Hitachi, Japan) at an operating voltage of 120 kV. The hydrodynamic diameter of the microspheres was characterized by laser particle size analyzer. (Zetasizer Nano ZS; Malvern, the UK).

2.8. In vitro release of SDF-1α

GelMA-1% imid hydrogel with 500 ng/mL PDA@SDF-1α (GelMA-imid/SDF-1α) was used to analyze the *in vitro* release behavior of SDF-1α. 1 mL of the GelMA-imid/SDF-1α hydrogel crosslinked with blue light was immersed in 5 mL of the PBS buffer and shaken at 37 °C. Take out the sustained-release solution at the indicated time points and stored at −80 °C, then 5 mL of the fresh PBS buffer was added. The whole release test was kept for 7 days. Finally, the concentration of SDF-1α was test by Human CXCL12/SDF-1 ELISA kit (PeproTech, USA) following the manufacturer's instructions.

2.9. In vitro cytotoxicity

Human amniotic mesenchymal stromal cells (hAMSCs) cultured in DMEM/F12 with 10% fetal bovine serum and 1% penicillin-streptomycin were used to assess the *in vitro* cytotoxicity of hydrogels [29]. The GelMA-imid pre-solution (50 μL) was firstly added in to 96-well plates, then exposed to blue light for 30 s to form hydrogel. Wash the hydrogel with PBS for three times. Then, 100 μL of the hAMSCs grown in the exponential phase was seeded on the hydrogel (1×10^4 per well) and cultured at 37 °C in a 5% CO_2 humidified incubator. After culturing for 24 h and 48 h, the culture medium was removed and refreshed with 100 μL of fresh culture medium containing 10% CCK-8 regent. Then the well plate was incubated in a cell culture incubator for 1 h. The absorbance value (OD value) at a wavelength of 450 nm was measured by a microplate reader (Multiskan MK3; Thermo scientific, USA).

2.10. Scratch experiments and in vitro hAMSCs differentiation

The effect of SDF-1α on the migration capacity of hAMSCs was evaluated by scratch wound healing assay [29,30]. The sterilized hydrogel was immersed in DEME/F12 complete medium at 37 °C for 24 h to obtain extract solution. hAMSCs were seeded into a 24-well plate with a DMEM/F12 complete medium. When cell's confluence reached over 90%, a scratch wound was generated in the cell monolayers with a sterile plastic 20 μL micropipette tip. The cells were allowed to growth for an additional 24 h with GelMA-imid/SDF-1α hydrogel extract solution. Photographs of scratch were taken at 0 h, 6 h, 12 h, and 24 h on an inverted microscope (Mshot, MI52). DMEM/F12 complete medium served as control.

hAMSCs of the P3 generation were seeded at a density of 1×10^6 per well in a 6-well plate with a cover glass. Incubated for 24 h until the cells adhere to the glass, and replace the culture medium with hydrogel extract: GelMA-imid hydrogel and GelMA-imid/SDF-1α hydrogel. DMEM/F12 complete medium served as control. After cultured for 3 d, the cells were fixed with paraformaldehyde and labeled with Nestin and GFAP by immunofluorescence.

2.11. In vivo cryogenic injury model and histological studies

Animal experiments were approved by the Experimental Animal Welfare and Ethics Management Committee of Southern Medical University and were executed in accordance with national guidelines and regulations. 45 male Sprague Dawley (SD) rats (8–11 weeks) were randomly divided into the following 5 groups (n = 3): (a) Control, (b) GelMA-imid hydrogel, (c) GelMA-imid/SDF-1α hydrogel, (d) GelMA-imid/hAMSC hydrogel, (e) GelMA-imid/SDF-1α/hAMSC hydrogel.

Rats were weighed and anesthetized by intraperitoneal injection with sodium pentobarbital (30 mg/kg). Shaved the hair of rat's head and disinfected with iodine. A midline sagittal incision was made to expose the skull of the rats. A circular dental drill was used to open the skull after the coronary suture, before the herringbone suture, and on the right side of the sagittal suture. The diameter of bone window was 5 mm. A copper rod with a diameter of 5 mm was pre-cooled in liquid nitrogen for 5 min, and the rod was placed on the exposed parietal skull for 60 s to make an injury. Hydrogel (20 μL) was injected into the center of damaged area using a 26 G syringe and maintained for 60 s to prevent the hydrogel from being squeezed out, whereas the control group were not treated with hydrogel. The bone window was fixed with bone wax and the wound was closed using suture needle after the injury [1]. All the operated rats were kept for recovery and were sacrificed at two different time points post injury (7 and 14 d). Seven days after operation, the isolated brains were fixed with paraformaldehyde and embedded in paraffin. Fourteen days after operation, half of the isolated brains in each group were fixed with paraformaldehyde, and the other half was stored at −80 °C were kept in −80 °C for Western blot analysis.

2.12. Statistical analysis

The WB data was analyzed using Image J software. Origin 9.0 and GraphPad Prism 7.0 were used to calculate various spectroscopic data and bar diagram. All experiments were repeated three times and results expressed as mean values ± standard errors (SD). The experiment data were analyzed using Analysis of Variance (ANOVA). The value of $^{*}p < 0.05$, $^{**}p < 0.01$ and $^{***}p < 0.001$, n = 3 was considered statistically significant.

3. Results and discussion

3.1. Chemical construction of hydrogels

Thiol-ene click chemistry can efficiently add small molecules containing thiol groups to macromolecules containing double bonds [25,26]. This reaction has a higher reaction rate in the presence of a photo-initiator. Therefore, 2-mercapto-1-methylimidazole was grafted to the main chain of GelMA using click chemistry while forming the hydrogel. The Fourier transform infrared (FTIR) spectra of GelMA and GelMA-imid (0.5%, 1%, 2%) were shown in Fig. 1 (A). The characteristic absorption peak of the *C*–S bond at 700 cm^{-1} indicated that the thiol group was added to the C═C double bond, thus proving the successful adding of 2-mercapto-1-methylimidazole to the main chain of GelMA.

3.2. Rheological, mechanical properties, in vitro degradation, and sustained release of SDF-1α

The rheological properties of GelMA and GelMA-imid hydrogel, grafted with different mass concentrations of 2-mercapto-1-methylimidazole, were presented in Fig. 1 (B) and 1 (C), respectively. The time-sweep sequence (Fig. 1 (B)) showed that the hydrogels completely formed under blue light crosslinking. The storage moduli (*G′*) and loss moduli (*G″*) of hydrogels were stable as time changed, and *G′* in all groups were maintained at 60–110 Pa. The introduction of imidazole groups caused the reduction of the *G'*. This may be due to that the C═C double bond on GelMA used for photo-crosslinking reacted with thiol group on 2-mercapto-1-methylimidazole, therefore decreasing the crosslinking density of GelMA. Though some of the C═C double bonds on the main chain of GelMA molecule reacted with thiol groups, the G′ of GelMA-imid hydrogel didn't show a significantly decrease. This may be explained by that the nitrogen atom in the imidazole group has a strong hydrogen bonding coordination effect [31,32], so the hydrogel network can still maintain a certain strength through hydrogen bonding.

The frequency-sweep sequence (Fig. 1 (C)) showed that loss moduli (*G″*) of hydrogels increased as the angular frequency increasing in all groups. However, the inflection points of *G"* of the GelMA-imid hydrogels were higher than that of GelMA, indicating that GelMA-imid hydrogels were more stable than GelMA hydrogel. This may due to the more hydrogen bonding coordination of GelMA-imid hydrogel, and thereby more resistance to deformation under high shear rate [31].

Fig. 1 (D) showed the static compressed stress-strain curve of hydrogels. The strain of GelMA-imid hydrogels was lower than GelMA under the same stress, which indicated that the deformation of GelMA-imid hydrogels was less after injection into the brain, and would be not easy to be extruded due to the compression of the surrounding tissue. No significant difference was found in the *in-vitro* degradation rates in PBS between GelMA and GelMA-imid hydrogel. They could all completely degrade after seven days (Fig. 1 (E)).

The release of SDF-1α was related to the degradation of hydrogel. As shown in Fig. 1(F), a fast release of SDF-1α was detected from 4 days, which was complied with the degradation of hydrogel. Due to the diffusion effect of SDF-1α and the degradation of hydrogel, SDF-1α had a faster release rate in the first four days. In addition, there were electrostatic forces [33] and non-covalent bonding between PDA and SDF-1, so that SDF-1α could not be released quickly on the first day, which prolonged the action time of SDF-1.

The human brain tissue has a *G'* range from 140 to 620 Pa [16], Matthew find that the hydrogel can maintain tight apposition to brain tissue if the hydrogel modulus is similar to the brain. Besides, previous reports believed that the mechanical strength of hydrogel will regulate stem cell fate, finally induced to different types of tissue [34]. Bone mesenchymal stem cells (BMSCs) cultured on hydrogel with the modulus between 0.1 and 1.0 kPa will differentiate into nerve cells. According to the rheological results, the GelMA-1% imid hydrogel we prepared was suitable for culturing hAMSCs and inducing them into nerve cells.

3.3. Shear thinning behavior

The repair efficiency of drug and stem cell therapy for treating TBI was dramatically compromised by blood-brain barrier (BBB) [3]. The effective amounts of drugs and nutrients transported by intravenous injection to the injured area will be greatly reduced due to BBB. Injectable hydrogel is highly suitable to treat TBI since it may enable a direct action of drug in the injured area and minimize the damage during administration [1,35]. In order to verify the injectability of GelMA-1% imid hydrogel, we tested its viscosity when the shear rate was changed between 0.1 Hz and 100 Hz. When the shear rate was 0.1 Hz, the viscosity was close to 18 Pa s^{-1}, while at a high shear rate of 100 Hz, the viscosity rapidly decreased to 0 Pa s^{-1}, and the viscosity gradually increases after applying lower shear rate (Fig. 1 (F)). This showed that the GelMA-1% imid hydrogel had shear thinning property and could be directly applied to damaged tissues through a syringe. Fig. 1 (H) showed a word “BRAIN” written by GelMA-1% imid hydrogel through a 26 G syringe.

3.4. Morphology of hydrogel and nanoparticles

The SEM images of GelMA and GelMA-imid hydrogels were shown

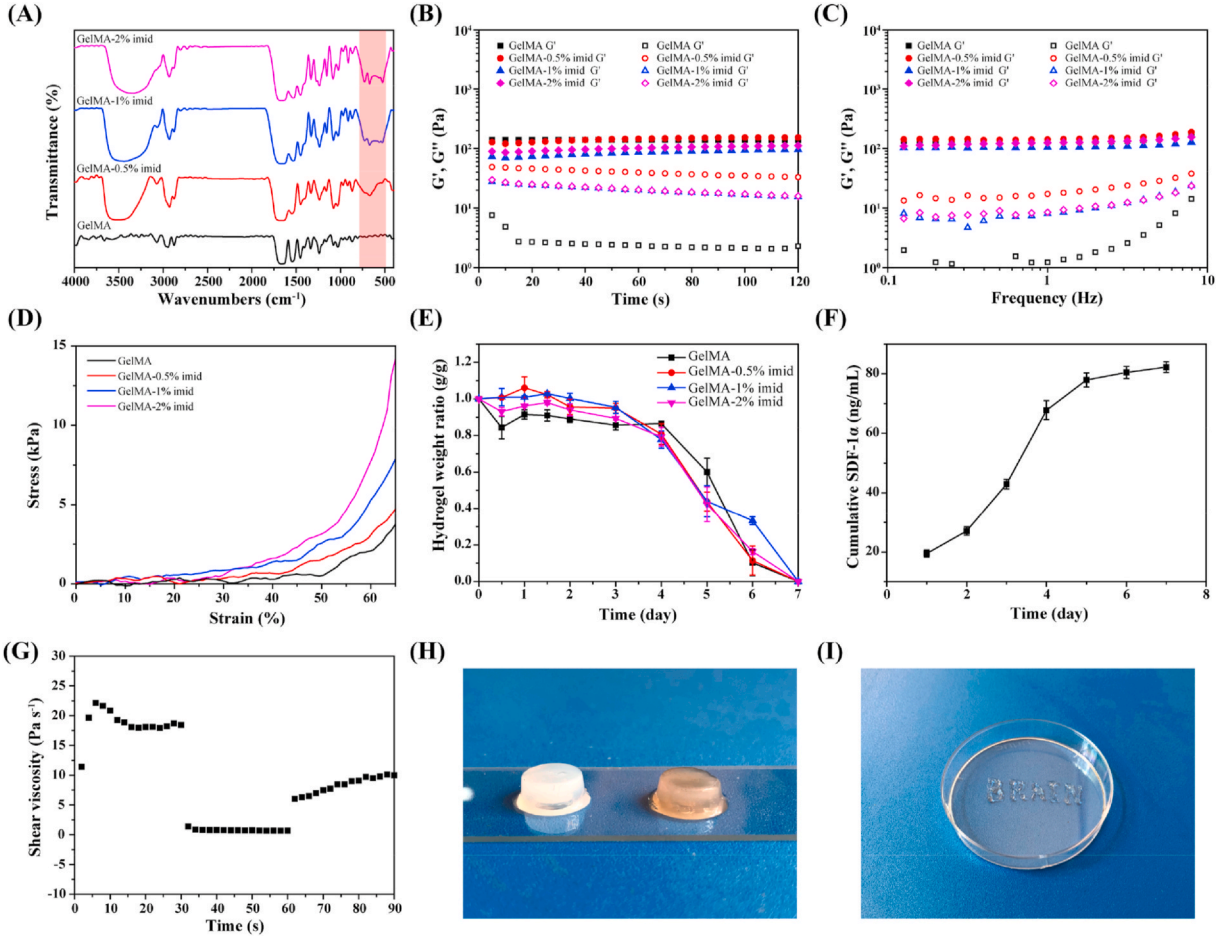

Fig. 1. Chemical construction, rheological and mechanical characterization of the hydrogel. (A) FTIR spectra of GelMA and GelMA-imid at different concentrations. (B) Time-sweep sequence of hydrogel. (C) Frequency-sweep sequence of hydrogel. (D) Stress-strain curve of hydrogel. (E) *In vitro* degradation behavior of hydrogel in PBS. (F) *In vitro* release curve of SDF-1α. (G) Shear-thinning properties characterized by viscosity change (shear rate 0.1 and 100 Hz). (H) Hydrogel appearance (Left: GelMA-imid hydrogel; Right: GelMA-imid/SDF-1α/hAMSCs hydrogel). (I) "Brain" written by hydrogel through a 26G needle.

in Fig. 2 (A). As can be seen from the figure, all the four groups could form network structure with uniform pore size. The average pore sizes of GelMA, GelMA-0.5% imid, GelMA-1% imid and GelMA-2% imid hydrogel were 176.6 ± 21.8 nm, 184.8 ± 26.7 nm, 204.6 ± 41.4 nm and 241.0 ± 34.5 nm, respectively. The pore size of the hydrogels after freeze-drying may be influenced by lyophilization condition [36]. But the average pore size distribution of the hydrogels we obtained after freeze-drying under the same conditions could roughly show the difference in crosslinking density. The gradually enlarged pore size may be due to the lower crosslinking density of GelMA-imid hydrogel. High concentration of 2-mercapto-1-methylimidazole might prohibit the crosslinking of C═C double bond on GelMA, thus leading to larger pore size.

The TEM images showed that the PDA and PDA@SDF-1α nanoparticles we prepared were spherical with uniform particle size (Fig. 2 (B)). By statistical analysis of TEM images, the particle size of PDA nanoparticles and PDA@SDF-1α nanoparticles were 130.36 ± 18.85 nm and 138.11 ± 18.55 nm, respectively, which was basically close to the particle size distribution obtained by the DLS. Because the SDF-1α was coated on the surface of PDA nanoparticles, so the PDA@SDF-1α nanoparticles had a larger size.

3.5. *In vitro* cytotoxicity, migration, and differentiation ability of hAMSCs

We had successfully grafted 2-mercapto-1-methylimidazole on the GelMA molecules and obtained GelMA-imid hydrogels. The *in-vitro* cytotoxicity of GelMA-imid hydrogel was performed to screen out the optimal concentration of 2-mercapto-1-methylimidazole. The cell viability of hAMSC co-cultured with hydrogel for 24 h and 48 h was shown in Fig. 3 (A). With the increase of the imidazole group content, the cytotoxicity also showed an increasing trend, but the overall survival rate was maintained above 80%, indicating that the hydrogel had no significant cytotoxicity. All the five groups showed an increased trend in cell viability at 48 h. GelMA hydrogel always possesses the highest cell viability due to its excellent biocompatibility. The possible reason for the decrease in cell viability was that as the concentration of 2-mercapto-1-methylimidazole increased, the content of free small molecules that have not been grafted onto GelMA through click chemistry also increased. These free 2-mercapto-1-methylimidazole molecules may increase cytotoxicity. Therefore, the toxicity of GelMA-2% imid hydrogel was significantly higher than the other three groups. In the end, we chose GelMA-1% imid hydrogel for subsequent experiments. The GelMA-1% imid hydrogel had a cell survival rate of 87.7% at 24 h and contains more imidazole groups, which could improve the biological function of the hydrogel [16,22].

Stem cells play an important role in the process of tissue regeneration. As a pluripotent stem cell, hAMSCs can differentiate into nerve cells so as to repair damaged nerve tissue [6,7]. Scratch test was performed to determine whether the addition of SDF-1α could promote the migration of hAMSC (Fig. 3 (B)). Images showed that SDF-1α at a concentration of 50 ng/mL could significantly increase the migration rate of hAMSC, completely covering the scratches after 24 h. This result

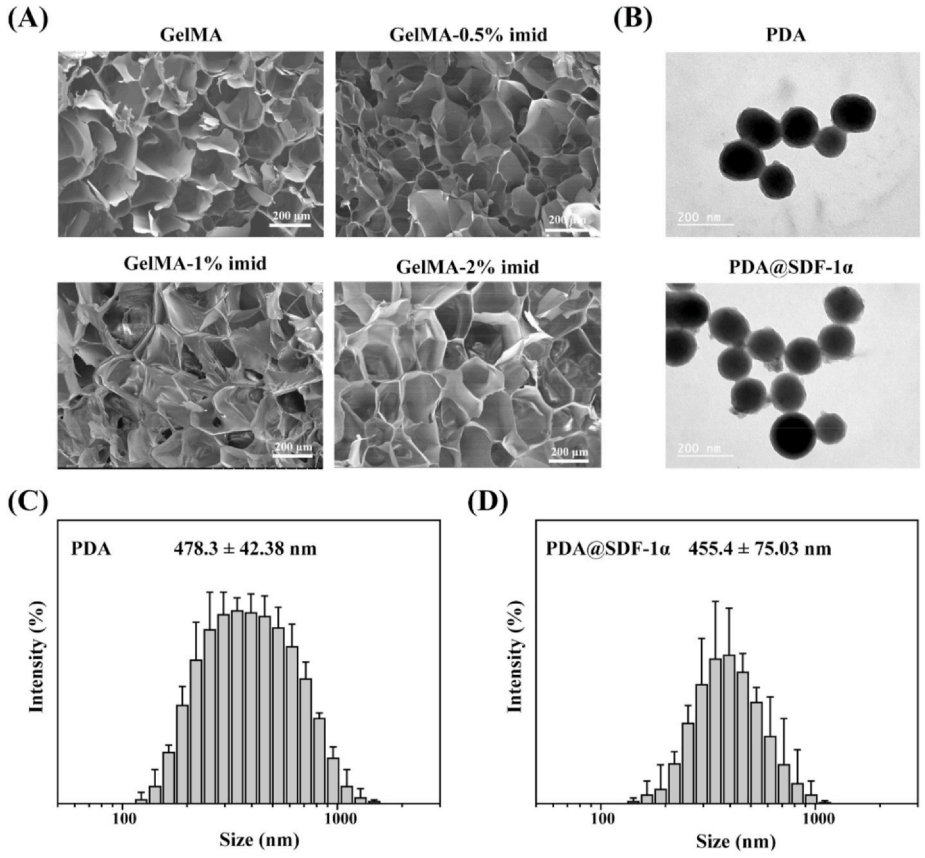

Fig. 2. (A) SEM image of lyophilized hydrogel. (B) TEM images of PDA and PDA@SDF-1α. (C) and (D) DLS of PDA and PDA@SDF-1α.

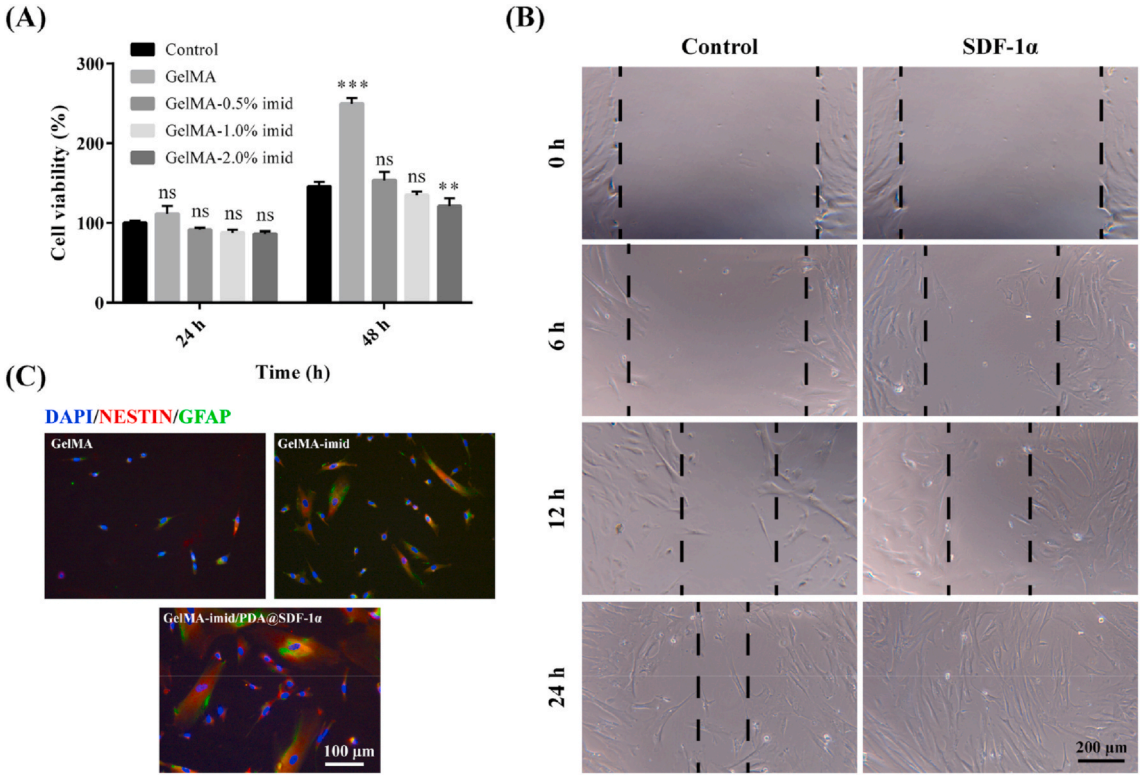

Fig. 3. (A) *In vitro* cytotoxicity of hAMSC cultured with GelMA-imid hydrogel. (B) Cell scratch experiment of SDF-1α. (C) *In vitro* differentiation of hAMSCs induced by GelMA and GelMA-imid hydrogel.

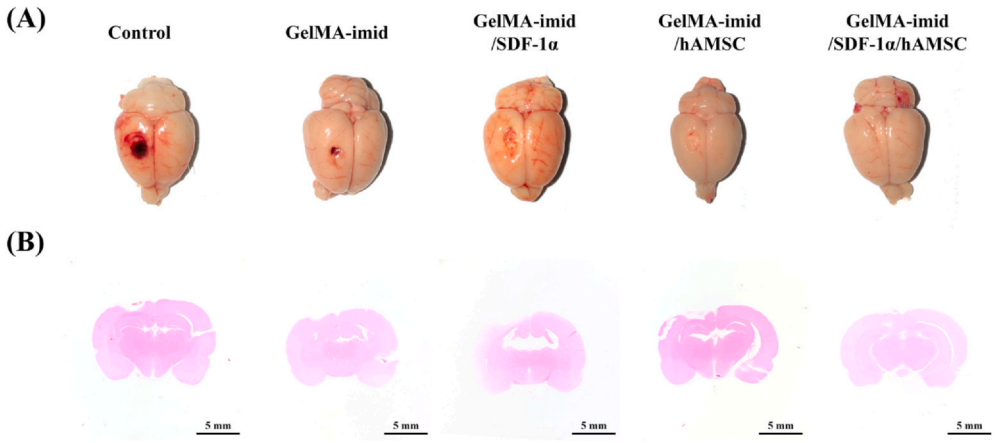

Fig. 4. (A) Images of rat brain after 14 days of treatment. (B) H&E staining of sagittal plane of brain tissue at 14 days.

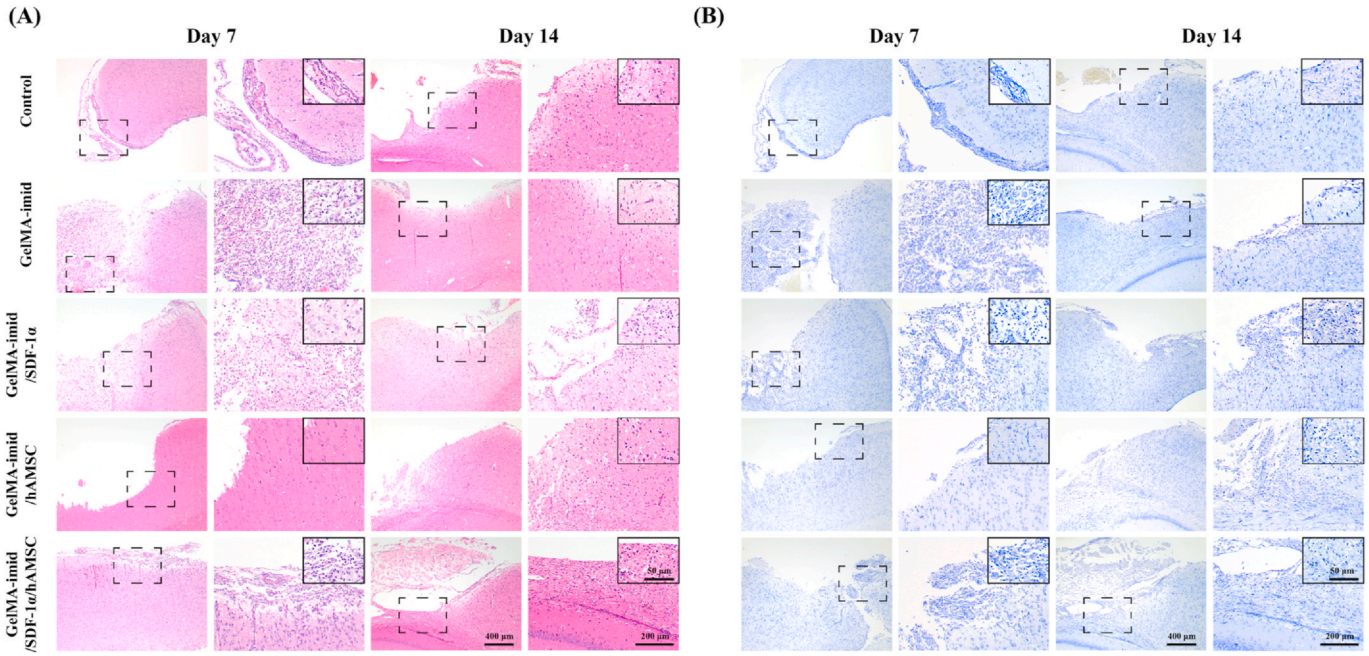

Fig. 5. (A) H&E stained images of cerebral cortex on days 7 and 14. (B) Toluidine blue stained images of cerebral cortex on days 7 and 14. (For interpretation of the references to colour in this figure legend, the reader is referred to the Web version of this article.)

indicated that SDF-1α could facilitate the homing of hAMSCs, accelerate the migration of stem cells from the surrounding area to the injured area, and promote injured tissue remodeling [10,11].

Small molecule inducers play an important role in stem cell differentiation. Many tri-substituted imidazole molecules have been reported to promote the neural differentiation of human pluripotent stem cells 9 days post treatment [21]. We also verified whether imidazole group and SDF-1α in GelMA-imid/SDF-1α hydrogel could promote hAMSC differentiation, and the results were shown in Fig. 3 (C) hAMSC were co-cultured with GelMA, GelMA-imid, and GelMA-imid/PDA@SDF-1α hydrogel extracts for 3 days, then immunofluorescence staining was performed to label the Nestin and glial fibrillary acidic protein (GFAP) of the cultured cells. Cells labeled with both red (Nestin) and green fluorescence (GFAP) indicated that the treated hAMSCs had the characteristics of nerve cells. The hAMSCs treated with GelMA-imid/PDA@SDF-1α hydrogel showed the highest Nestin (+) and GFAP (+) and the cells represented an elongated morphology. These results indicated that the GelMA-imid/PDA@SDF-1α hydrogel had the best induction effect, which might promote the regeneration and functional reconstruction of brain tissue.

3.6. Histological analysis of in vivo cryogenic brain injury

Images of injured brain treated with different hydrogels for 14 days after injury were displayed in Fig. 4 (A), and the related sagittal H&E staining images were shown in Fig. 4 (B). As shown in the figures, the circular defect caused by copper rod in Control group was the largest. At the same time, a large amount of blood stasis was also seen in Control group. GelMA-imid hydrogel treatment group had no obvious blood stasis, but there were still large defects. The brains of both the GelMA-imid/SDF-1α and GelMA-imid/hAMSC hydrogel treated groups still had defects, but the defects were much smaller than those in Control group and GelMA-imid hydrogel treated group. The damage in GelMA-imid/SDF-1α/hAMSC hydrogel treated group was almost invisible in days 14. The corresponding sagittal H&E staining images were also roughly the same as those in Fig. 4 (A). Except for the GelMA-imid/SDF-1α/hAMSC hydrogel treated group, significant hollows were observed in the gray matter at the upper left of the brain in Control, GelMA-imid, GelMA-imid/SDF-1α and GelMA-imid/hAMSC groups.

Fig. 5 showed the results of H&E and toluidine blue staining of the cerebral cortex. It can be seen from the H&E staining that there were a

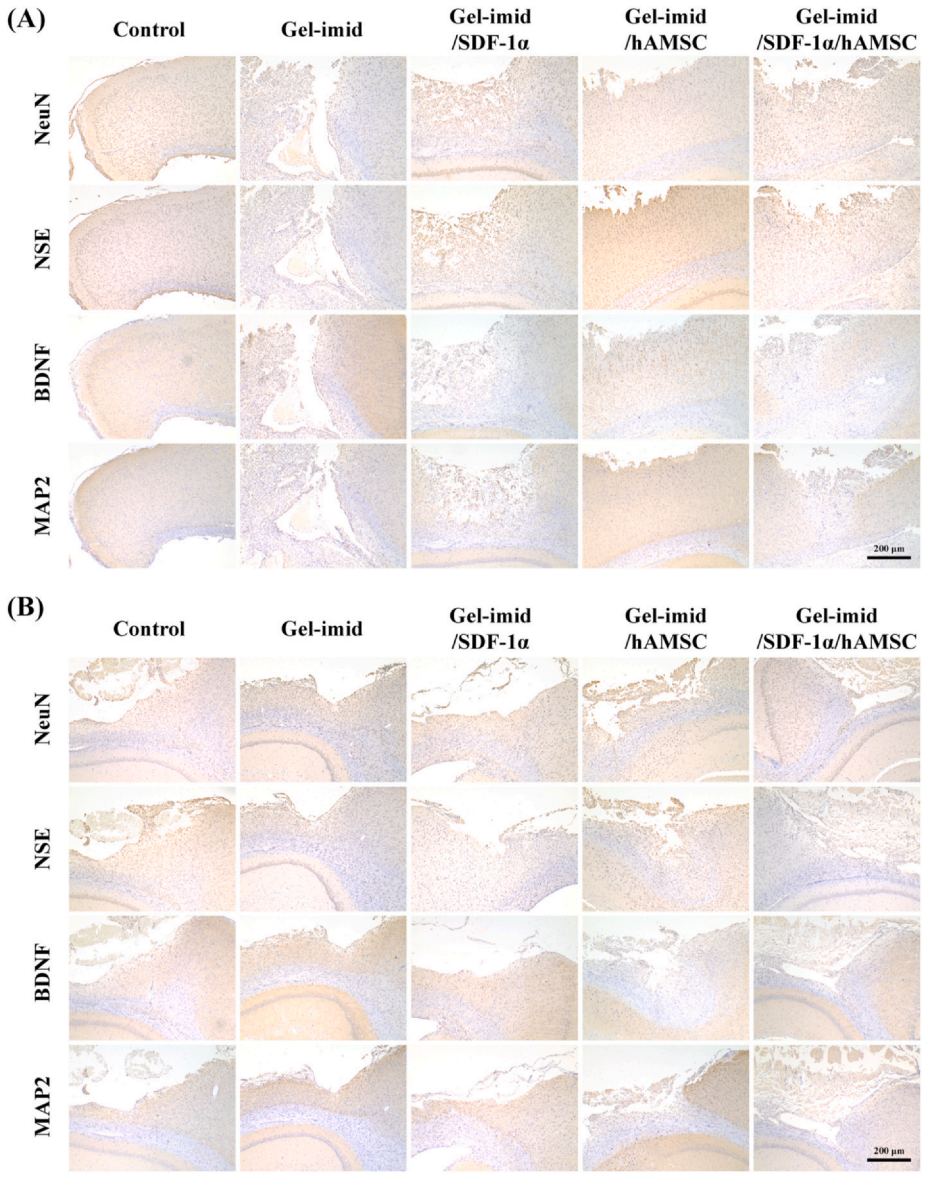

Fig. 6. (A) Immunohistochemical staining of NeuN, NSE, BNDF and MAP2 in the damaged brain tissues in days 7. (B) Immunohistochemical staining of NeuN, NSE, BNDF and MAP2 in the damaged brain tissues in days 14.

large number of defects in the Control group on the 7th day, and the middle cortex was broken due to injury. The number of glial cells around the injured area in the hydrogel treatment group was significantly more than that in the control group. Glial cell after brain injury can proliferate to fill the defect site as well as secrete neurotrophic factors and various growth factors to promote tissue regeneration. Glial cell line-derived neurotrophic factor (GDNF) is crucially important for the development and maintenance of brain tissue. As an important neuroprotective therapeutic candidate, it has been widely used to treat Parkinson's disease [37]. The H&E staining results indicated that the GelMA-imid/SDF-1α/hAMSC hydrogel could significantly promote the proliferation of glial cells in the early stage of injury, which might produce GDNF to maintain and regenerate brain tissue. Since we only conducted a short-term (14 days) experiment, further experiments are still needed to be explored whether glial scars will form with the extension of treatment time.

Toluidine blue can be used to dye the Nissl body. The coloured Nissl body appears blue-violet oval or triangular [1,38]. Nissl bodies are present in neurons and are responsible for protein synthesis. A decrease in the number of Nissl bodies represents a decline in neural tissue function [1,38]. Fig. 5 (B) showed that the Control group had the lowest amount of Nissl bodies, the GelMA-imid/SDF-1α/hAMSC hydrogel group had the highest amount, and GelMA-imid/SDF-1α and GelMA-imid/hAMSC hydrogel groups had similar numbers of Nissl bodies. These findings might be due to the synergistically promoting effect of imidazole and SDF-1α on the differentiation of hAMSCs into neural stem cells. Besides, SDF-1α could recruit peripheral neural stem cells to homing, and the differentiated hAMSC could jointly promote the repair of damaged tissues.

3.7. Immunohistochemistry and WB analysis

Mature neuronal cell bodies are identified by expressing neuron-specific nuclear protein (NeuN), neuron-specific enolase (NSE) and microtubule associated protein 2 (MAP2) [2]. NeuN exists in most neuronal cells and NSE is expressed by mature neurons. MAP2 is important in microtubule assembly. These three proteins were commonly used to determine neuronal cell type. We performed immunohistochemical staining of NeuN, NSE, BDNF and MAP2 in the damaged brain tissues, and the results were shown in Fig. 6. The

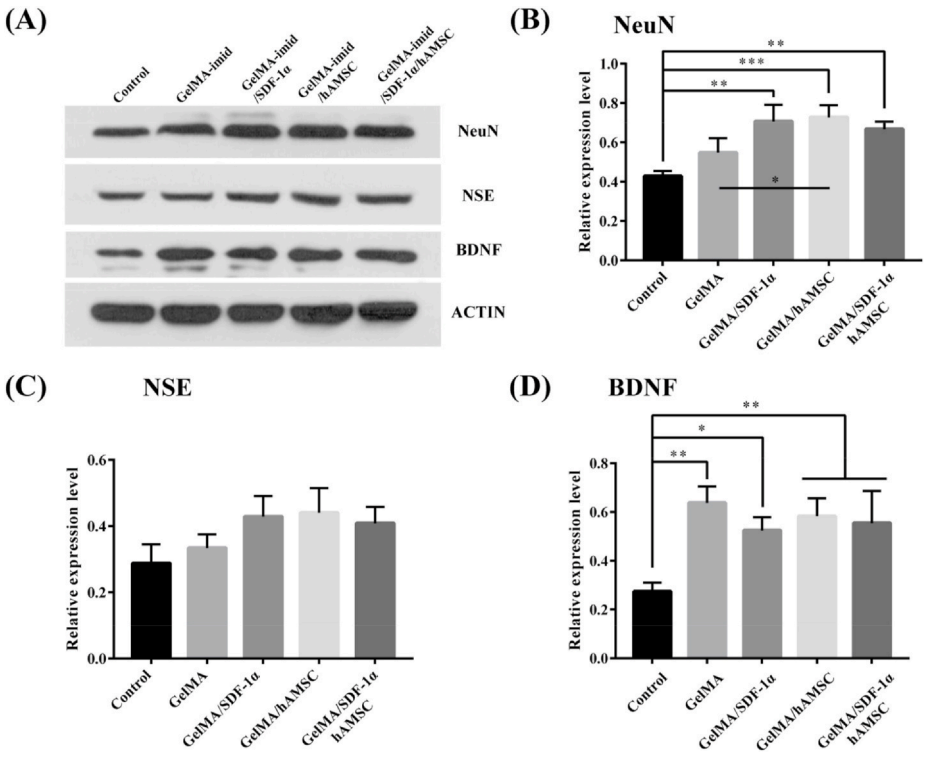

Fig. 7. (A) WB image and (B) relative value of cerebral cortex in the injured area. The unmarked indicates no significant difference.

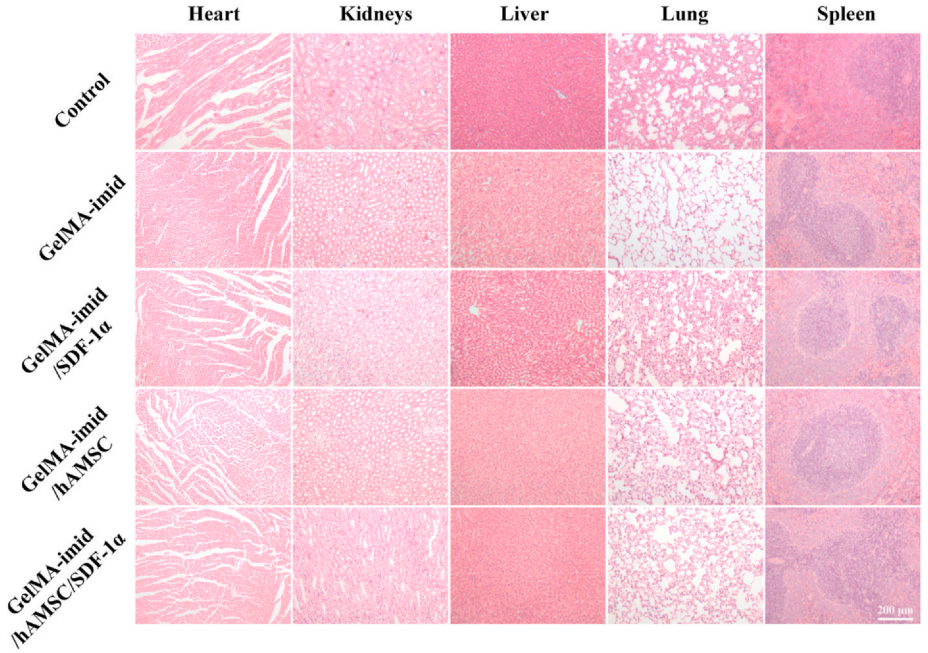

Fig. 8. H&E staining of heart, liver, spleen, lung and kidney after 14 days of treatment in rats.

GelMA-imid/SDF-1α/hAMSC hydrogel group had the highest positive expression of NeuN, NSE, BDNF and MAP2, and their expression levels at 14 days was higher than that on the 7th day.

Then, Western blot was performed on the 14th day for semi-quantitative analysis of the related protein (NeuN, NSE and BDNF) and the results were shown in Fig. 7. The relative expression level of NeuN, NSE and BDNF in the hydrogel treated groups were higher than that in the Control group. The NSE and NeuN had high expression in GelMA-imid/SDF-1α, GelMA-imid/hAMSC and GelMA-imid/SDF-1α/hAMSC hydrogel group, showing that those hydrogels-treated groups had more mature neurons, which was consistent with the results in *vitro* cell proliferation results. Our results suggested that the GelMA-imid/SDF-1α/hAMSC hydrogel resulted in more mature neurons to recover the TBI-damaged brain tissues.

3.8. *In vivo toxicity analysis of main organs*

In order to determine whether the GelMA-imid hydrogel penetrated the blood-brain barrier and caused systemic cytotoxicity, we performed H&E staining analysis on the main organs (heart, liver, spleen, lung,

kidney) on day 14 (Fig. 8). No damage to the tissue morphology and organ structure of each internal organ was observed in all the groups, indicating that the materials used in the experiment did not cause any physiological toxicity to the rats.

4. Conclusion

In this study, we prepared 2-mercapto-1-methylimidazole grafted GelMA-imid hydrogel, and loaded with PDA@SDF-1α nanoparticles and hAMSCs. The imidazole groups in GelMA-imid hydrogel synergistically worked with SDF-1α to promote the migration and differentiation of hAMSCs. The GelMA-1% imid hydrogel had a low module (95 Pa), high compression stress (5.2 kPa) and could be completely degraded (Fig. 1), which was suitable for treating brain damage. The *in-vitro* cell scratch and differentiation experiments of GelMA-imid/SDF-1α/hAMSCs hydrogel showed that the imidazole groups and SDF-1α could promote the migration of hAMSCs to injury site and directionally differentiation into nerve cells. For treating cryogenic brain injury, the GelMA-imid/SDF-1α/hAMSCs hydrogel treated group showed the smallest injured area and least decrease of Nissl body. Immunohistochemistry and WB analyses also presented the highest relevant protein expression levels of neuron. The GelMA-imid/SDF-1α/hAMSCs hydrogel may provide a new clinical option to treat TBI.

Credit author contribution statement

Yantao Zheng: Resources, Writing - original draft, preparation. **Gang Wu:** Resources, Writing - original draft, preparation. **Limei Chen:** Resources. **Ying Zhang:** Methodology. **Yuwei Luo:** Resources. **Yong Zheng:** Methodology. **Fengjun Hu:** Validation. **Haiyan Lin:** Conceptualization, Investigation, Writing - review & editing. **Bin Liu:** Conceptualization, Investigation, Writing - review & editing.

Declaration of competing interest

The authors declare no competing financial interest.

Acknowledgments

This work was financially supported by the Science and Technology Project of Guangdong Province (No. 2015A020212021), Medical Health Science and Technology Project of Zhejiang Provincial Health Commission (No. 2020KY625), Zhejiang Provincial Department of Education (No. Y201636248), Natural Science Foundation of Zhejiang Province (No. LQY17H140023) Science Technology Department of Zhejiang Province (No. 2017C33168), Zhejiang Provincial Basic Public Welfare Research Project (No. GJ19H140001) and China's National Key R&D Programs (No. 2018YFB0407204).

References

[1] K. Pradhan, G. Das, U. Khan, V. Gupta, S. Barman, A. Adak, S. Ghosh, Neuro-Regenerative choline-functionalized injectable graphene oxide hydrogel repairs focal brain injury, ACS Chem. Neurosci. 10 (3) (2019) 1535–1543.
[2] K. Zhang, Z.Q. Shi, J.K. Zhou, Q. Xing, S.S. Ma, Q.H. Li, Y.T. Zhang, M.H. Yao, X.F. Wang, Q. Li, J.A. Li, F.X. Guan, Potential application of an injectable hydrogel scaffold loaded with mesenchymal stem cells for treating traumatic brain injury, J. Mater. Chem. B 6 (19) (2018) 2982–2992.
[3] H. Ghuman, C. Mauney, J. Donnelly, A.R. Massensini, S.F. Badylak, M. Modo, Biodegradation of ECM hydrogel promotes endogenous brain tissue restoration in a rat model of stroke, Acta Biomater. 80 (2018) 66–84.
[4] M. Modo, S.F. Badylak, A roadmap for promoting endogenous in situ tissue restoration using inductive bioscaffolds after acute brain injury, Brain Res. Bull. 150 (2019) 136–149.
[5] A.J. Jahan-Abad, S.S. Negah, H.H. Ravandi, S. Ghasemi, M. Borhani-Haghighi, W. Stummer, A. Gorji, M.K. Ghadiri, Human neural stem/progenitor cells derived from epileptic human brain in a self-assembling peptide nanoscaffold improve traumatic brain injury in rats, Mol. Neurobiol. 55 (12) (2018) 9122–9138.
[6] C. Giampa, A. Alvino, M. Magatti, A.R. Silini, A. Cardinale, E. Paldino, F.R. Fusco, O. Parolini, Conditioned medium from amniotic cells protects striatal degeneration and ameliorates motor deficits in the R6/2 mouse model of Huntington's disease, J. Cell Mol. Med. 23 (2) (2019) 1581–1592.
[7] H.L. Zhou, X.J. Zhang, M.Y. Zhang, Z.J. Yan, Z.M. Xu, R.X. Xu, Transplantation of human amniotic mesenchymal stem cells promotes functional recovery in a rat model of traumatic spinal cord injury, Neurochem. Res. 41 (10) (2016) 2708–2718.
[8] F. Pischiutta, L. Brunelli, P. Romele, A. Silini, E. Sammali, L. Paracchini, S. Marchini, L. Talamini, P. Bigini, G.B. Boncoraglio, R. Pastorelli, M.G. De Simoni, O. Parolini, E.R. Zanier, Protection of brain injury by amniotic mesenchymal stromal cell-secreted metabolites, Crit. Care Med. 44 (11) (2016) E1118–E1131.
[9] K. Fujita, K. Tatsumi, E. Kondoh, Y. Chigusa, H. Mogami, T. Fujii, S. Yura, K. Kakui, I. Konishi, Differential expression and the anti-apoptotic effect of human placental neurotrophins and their receptors, Placenta 32 (10) (2011) 737–744.
[10] X.T. He, X. Li, Y. Xia, Y. Yin, R.X. Wu, H.H. Sun, F.M. Chen, Building capacity for macrophage modulation and stem cell recruitment in high-stiffness hydrogels for complex periodontal regeneration: experimental studies in vitro and in rats, Acta Biomater. 88 (2019) 162–180.
[11] W.H. Jian, H.C. Wang, C.H. Kuan, M.H. Chen, H.C. Wu, J.S. Sun, T.W. Wang, Glycosaminoglycan-based hybrid hydrogel encapsulated with polyelectrolyte complex nanoparticles for endogenous stem cell regulation in central nervous system regeneration, Biomaterials 174 (2018) 17–30.
[12] L.L. Cui, H.L. Qu, T. Xiao, M. Zhao, J. Jolkkonen, C.S. Zhao, Stromal cell-derived factor-1 and its receptor CXCR4 in adult neurogenesis after cerebral ischemia, Restor. Neurol. Neurosci. 31 (3) (2013) 239–251.
[13] Q. Dai, H.M. Geng, Q. Yu, J.C. Hao, J.W. Cui, Polyphenol-based particles for theranostics, Theranostics 9 (11) (2019) 3170–3190.
[14] M.H. Yao, F. Gao, R. Xu, J.N. Zhang, Y.H. Chen, F.X. Guan, A dual-enzymatically cross-linked injectable gelatin hydrogel loaded with BMSC improves neurological function recovery of traumatic brain injury in rats, Biomater Sci-Uk 7 (10) (2019) 4088–4098.
[15] Q. Zhu, Y.H. Gong, T.W. Guo, J. Deng, J.G. Ji, B.C. Wang, S.L. Hao, Thermo-sensitive keratin hydrogel against iron-induced brain injury after experimental intracerebral hemorrhage, Int. J. Pharm. 566 (2019) 342–351.
[16] M.J. Rowland, C.C. Parkins, J.H. McAbee, A.K. Kolb, R. Hein, X.J. Loh, C. Watts, O.A. Scherman, An adherent tissue-inspired hydrogel delivery vehicle utilised in primary human glioma models, Biomaterials 179 (2018) 199–208.
[17] Q. Xu, A. Sigen, Y.S. Gao, L.R. Guo, J. Creagh-Flynn, D.Z. Zhou, U. Greiser, Y.X. Dong, F.G. Wang, H.Y. Tai, W.G. Liu, W. Wang, W.X. Wang, A hybrid injectable hydrogel from hyperbranched PEG macromer as a stem cell delivery and retention platform for diabetic wound healing, Acta Biomater. 75 (2018) 63–74.
[18] Y.X. Dong, A. Sigen, M. Rodrigues, X.L. Li, S.H. Kwon, N. Kosaric, S. Khong, Y.S. Gao, W.X. Wang, G.C. Gurtner, Injectable and tunable gelatin hydrogels enhance stem cell retention and improve cutaneous wound healing, Adv. Funct. Mater. 27 (24) (2017) 1606619.
[19] C.M. Chen, J.C. Tang, Y. Gu, L.L. Liu, X.Z. Liu, L.F. Deng, C. Martins, B. Sarmento, W.G. Cui, L. Chen, Bioinspired hydrogel electrospun fibers for spinal cord regeneration, Adv. Funct. Mater. 29 (4) (2019) 1806899.
[20] G. Eke, N. Mangir, N. Hasirci, S. MacNeil, V. Hasirci, Development of a UV cross-linked biodegradable hydrogel containing adipose derived stem cells to promote vascularization for skin wounds and tissue engineering, Biomaterials 129 (2017) 188–198.
[21] Q.X. Zhong, F. Laco, M.C. Liao, T.L. Woo, S.K.W. Oh, C.L.L. Chai, Influencing the fate of cardiac and neural stem cell differentiation using small molecule inhibitors of ALK5, Stem Cell Transl Med 7 (10) (2018) 709–720.
[22] L.T.A. Hong, Y.M. Kim, H.H. Park, D.H. Hwang, Y. Cui, E.M. Lee, S. Yahn, J.K. Lee, S.C. Song, B.G. Kim, An injectable hydrogel enhances tissue repair after spinal cord injury by promoting extracellular matrix remodeling, Nat. Commun. 8 (2017) 533.
[23] D.H. Hu, C.B. Liu, L. Song, H.D. Cui, G.H. Gao, P. Liu, Z.H. Sheng, L.T. Cai, Indocyanine green-loaded polydopamine-iron ions coordination nanoparticles for photoacoustic/magnetic resonance dual-modal imaging-guided cancer photothermal therapy, Nanoscale 8 (39) (2016) 17150–17158.
[24] K. Yue, G. Trujillo-de Santiago, M.M. Alvarez, A. Tamayol, N. Annabi, A. Khademhosseini, Synthesis, properties, and biomedical applications of gelatin methacryloyl (GelMA) hydrogels, Biomaterials 73 (2015) 254–271.
[25] N.Y. Ning, S. Wang, Z.T. Zhang, Z.B. Feng, Z.P. Zheng, B. Yu, M. Tian, L.Q. Zhang, Superhydrophobic coating with ultrahigh adhesive force and good anti-scratching on elastomeric substrate by thiol-ene click chemistry, Chem. Eng. J. 373 (2019) 318–324.
[26] N. Van Herck, D. Maes, K. Unal, M. Guerre, J.M. Winne, F.E. Du Prez, Covalent adaptable networks with tunable exchange rates based on reversible thiol-yne cross-linking, Angew. Chem. Int. Ed. 59 (9) (2020) 3609–3617.
[27] N. Monteiro, G. Thrivikraman, A. Athirasala, A. Tahayeri, C.M. Franca, J.L. Ferracane, L.E. Bertassoni, Photopolymerization of cell-laden gelatin methacryloyl hydrogels using a dental curing light for regenerative dentistry, Dent. Mater. 34 (3) (2018) 389–399.
[28] L. Wang, X.H. Zhang, K. Yang, Y.V. Fu, T.S. Xu, S.L. Li, D.W. Zhang, L.N. Wang, C.S. Lee, A novel double-crosslinking-double-network design for injectable hydrogels with enhanced tissue adhesion and antibacterial capability for wound treatment, Adv. Funct. Mater. 30 (1) (2019) 1904156.
[29] F.F. Zhou, Y. Hong, X.Z. Zhang, L. Yang, J. Li, D.M. Jiang, V. Bunpetch, Y.J. Hu, H.W. Ouyang, S.F. Zhang, Tough hydrogel with enhanced tissue integration and in situ forming capability for osteochondral defect repair, Appl Mater Today 13 (2018) 32–44.
[30] F. Fiorini, E.A. Prasetyanto, F. Taraballi, L. Pandolfi, F. Monroy, I. Lopez-Montero, E. Tasciotti, L. De Cola, Nanocomposite hydrogels as platform for cells growth, proliferation, and chemotaxis, Small 12 (35) (2016) 4881–4893.
[31] B.C. Liu, Y. Wang, Y. Miao, X.Y. Zhang, Z.X. Fan, G. Singh, X.Y. Zhang, K.G. Xu,

B.Y. Li, Z.Q. Hu, M. Xing, Hydrogen bonds autonomously powered gelatin methacrylate hydrogels with super-elasticity, self-heal and underwater self-adhesion for sutureless skin and stomach surgery and E-skin, Biomaterials 171 (2018) 83–96.
[32] Y.L. Yu, P.F. Li, C.L. Zhu, N. Ning, S.Y. Zhang, G.J. Vancso, Multifunctional and recyclable photothermally responsive cryogels as efficient platforms for wound healing, Adv. Funct. Mater. 29 (35) (2019) 1904402.
[33] B.P. Purcell, J.A. Elser, A.B. Mu, K.B. Margulies, J.A. Burdick, Synergistic effects of SDF-1 alpha chemokine and hyaluronic acid release from degradable hydrogels on directing bone marrow derived cell homing to the myocardium, Biomaterials 33 (31) (2012) 7849–7857.
[34] A.J. Engler, S. Sen, H.L. Sweeney, D.E. Discher, Matrix elasticity directs stem cell lineage specification, Cell 126 (4) (2006) 677–689.
[35] S.S. Negah, P. Oliazadeh, A.J. Jahan-Abad, A. Eshaghabadi, F. Samini, S. Ghasemi, A. Asghari, A. Gorji, Transplantation of human meningioma stem cells loaded on a self-assembling peptide nanoscaffold containing IKVAV improves traumatic brain injury in rats, Acta Biomater. 92 (2019) 132–144.
[36] I. Noshadi, S. Hong, K.E. Sullivan, E.S. Sani, R. Portillo-Lara, A. Tamayol, S.R. Shin, A.E. Gao, W.L. Stoppel, L.D. Black, A. Khademhosseini, N. Annabi, In vitro and in vivo analysis of visible light crosslinkable gelatin methacryloyl (GelMA) hydrogels, Biomater Sci-Uk 5 (10) (2017) 2093–2105.
[37] A.A. Ayanlaja, B.L. Zhang, G.Q. Ji, Y. Gao, J. Wang, K. Kanwore, D.S. Gao, The reversible effects of glial cell line-derived neurotrophic factor (GDNF) in the human brain, Semin. Canc. Biol. 53 (2018) 212–222.
[38] C.Y. Kuan, Y.Y. Lin, C.Y. Chen, C.C. Yang, C.Y. Chi, C.H. Li, G.C. Dong, F.H. Lin, The preparation of oxidized methylcellulose crosslinked by adipic acid dihydrazide loaded with vitamin C for traumatic brain injury, J. Mater. Chem. B 7 (29) (2019) 4499–4508.